学位論文（博士）

Assessment of the relationship between the hepatic contrast enhancement effect in the hepatobiliary phase and hepatic signal changes in free-breathing continuous multiphasic dynamic EOB-MRI

(圧縮センシングを用いた自由呼吸下での多相ダイナミック EOB-MRI における肝実質の信号の経時的変化と肝細胞相の造影効果との関連性の評価)

氏名　田邊　雅也

所属　山口大学大学院医学系研究科

医学専攻　放射線医学講座

令和 4 年 10 月

学位論文の関連論文の研究背景及び要旨

所属　放射線医学講座
氏名　田邊雅也

〔題名〕

Assessment of the relationship between the hepatic contrast enhancement effect in the hepatobiliary phase and hepatic signal changes in free-breathing continuous multiphasic dynamic EOB-MRI.

「圧縮センシングを用いた自由呼吸下での多相ダイナミック EOB-MRI における肝実質の信号の経時的変化と肝細胞相の造影効果との関連性の評価」

European Journal of Radiology 144 (2021) 109959

〔研究背景〕

Gd-EOB-DTPA を用いた肝臓 MRI において動脈相、門脈相、移行相、肝細胞相をそれぞれの時相で息止めをして撮像する手法は広く用いられており、肝病変の検出と評価に役立っている。加えて、肝細胞相における肝実質の信号強度と肝実質の線維化の程度とに相関関係があると報告する文献も散見され、EOB-MRI は肝機能評価においても有用である。

近年では圧縮センシングの登場により自由呼吸下における連続多相ダイナミック撮像が可能となり、肝実質の信号強度の変化を経時的に評価することができるようになった。しかしながら、肝実質の信号の経時的変化と肝細胞相の信号との関連について報告した文献はなかった。

本研究の目的は、多相ダイナミック撮像における肝実質の信号変化を評価するためのパラメータと肝細胞相の信号強度との関連を検討することである。

〔要旨〕

方法：

本研究は圧縮センシングを用いた自由呼吸下での多相ダイナミック EOB-MRI を撮像された 96 人の患者を対象とした。多相ダイナミック撮像として自由呼吸下で 11 秒毎に 1 相を 5 分間、脂肪抑制 T1 強調画像を撮像し、単純 1 相と造影 28 相を撮像した。造影剤投与後 20 分後に肝細胞相を撮像し、30 相目とした。ROI: region of intensity を肝右葉に 2 つ、左葉に 1 つを脈管を避けながら可能な限り大きく設定した。3 つの ROI の信号強度の平均値をそれぞれの時相の信号強度とした。

以下の増強効果のパラメータについて評価した。

CER (contrast enhancement ratio)

$CER_{y\text{-}x}$: $(SI_y - SI_x)/SI_x$（x 相目から y 相目)とし、

$CER_{4\text{-}pre}$：動脈相

$CER_{7\text{-}5}$：門脈相から動脈相にかけて

$CER_{7\text{-}pre}$：門脈相

$CER_{28\text{-}pre}$：5 分早期肝細胞相

$CER_{28\text{-}7}$：門脈相から 5 分早期肝細胞相

$CER_{HBP\text{-}pre}$：20 分肝細胞相

GRL (gradient of regression line)：回帰曲線の傾き
$GRL_{y\text{-}x}$: x 相目から y 相目とし、
$GRL_{4\text{-}2}$：動脈相での傾き
$GRL_{7\text{-}4}$ ：門脈相での傾き
$GRL_{7\text{-}2}$ ：動脈相、門脈相にかけての傾き
$GRL_{28\text{-}7}$：門脈相から早期肝細胞相での傾き

先行研究によると、肝実質の線維化の重症度(F0-F2 vs F3-F4)に基づいて $CER_{HBP\text{-}pre}$ で cut off 値を 0.703 として肝細胞相での増強効果が insufficient HBP enhancement group と sufficient HBP enhancement group に分けれるとしている。$CER_{HBP\text{-}pre}<0.703$ または $CER_{HBP\text{-}pre}>0.703$ により患者を 2 群に分け、$CER_{y\text{-}x}$、$GRL_{y\text{-}x}$ について検討した。
上記に加えて年齢、性別、総ビリルビン、プロトロンビン時間、アルブミン、eGFR についても、この 2 群間で比較した(ウィルコクソンの順位和検定)。
肝細胞相の増強効果に対する影響の大きさを調べるためにノンパラメトリック検定も用いられた(スピアマンの順位相関係数)。

結果：
動脈相(CER4-pre、GRL4-2)に関する結果として、これらは sufficient HBP enhancement group が insufficient HBP enhancement group の間に有意差を認めなかった。
動脈門脈相(1 相目～7 相目)に関する結果としては、CER7-pre は sufficient HBP enhancement group が insufficient HBP enhancement group より有意に高い値となった(0.55 vs 0.44, $p<0.001$)。CER4-pre、GRL4-2、Gradient7-4、Gradient7-2 では 2 群間に有意差は見られなかった。
5 分後の早期肝細胞相(1 相目～28 相目)に関する結果としては、CER28-pre、CER28-7、GRL28-7 において sufficient HBP enhancement group が insufficient HBP enhancement group より有意に高い値となった(0.64 vs 0.47, 0.10 vs 0.03, 1.27 vs 0.27、すべて $p<0.001$)。
血液データ(総ビリルビン、プロトロビン時間、アルブミン、eGFR)においても 2 群間で有意差が認められた($p=0.004$-0.049)。CER7-pre、CER28-pre、CER28-7、GRL28-7 の各パラメータは血液データのパラメータよりも相関係数が高かった。
CER28-pre が最も相関係数が高かった(0.838)。

考察：
動脈相では 2 群間(sufficient HBP enhancement group と insufficient HBP enhancement group)に有意差を認めず、門脈相のパラメータでは有意差が見られた。機序としては推測になってしまうが、肝の線維化の進行に伴い門脈血流は低下しやすいが、動脈血流は比較的保たれることが原因であろうか。

また、肝細胞相の信号強度は、血液データなどによって得られた肝機能を示す数値と相関するこ

とはこれまでにも報告されてきた。肝機能が良好であるほど、肝細胞が EOB を取り込みやすいためとされる。
本研究では腎機能と肝細胞相の信号強度とにも相関が見られたが、腎機能が低い症例の方がより肝排泄の割合が増えるからと思われた。
本研究のように、ダイナミック撮像中に得られるパラメータが肝細胞相における肝実質の信号強度と相関することを報告した研究はこれまでになかった。
CER7-pre、CER28-pre、CER28-7、GRL28-7 の各パラメータは、いずれも血液データのパラメータよりも相関係数が高かった。
本研究のようにダイナミック撮像中に得られたパラメータを用いれば、血液データよりも高い精度で肝実質の信号強度を予測することができる。
これにより、肝細胞相の撮像タイミングを症例により短縮できることが期待される。

結語：
圧縮センシングを用いた自由呼吸下での EOB-MRI のダイナミック撮像おいて、肝実質の信号強度の変化を連続データとして捉えることにより得られたパラメータは、肝細胞相での肝実質の信号強度と強い相関を示す。これにより、肝細胞相の撮像タイミングを症例により短縮できることが期待される。

European Journal of Radiology 144 (2021) 109959

Contents lists available at ScienceDirect

European Journal of Radiology

journal homepage: www.elsevier.com/locate/ejrad

Assessment of the relationship between the hepatic contrast enhancement effect in the hepatobiliary phase and hepatic signal changes in free-breathing continuous multiphasic dynamic EOB-MRI

Masaya Tanabe *, Masahiro Tanabe, Matakazu Furukawa, Etsushi Iida, Munemasa Okada, Katsuyoshi Ito

Department of Radiology, Yamaguchi University Graduate School of Medicine, Ube, Japan

ARTICLE INFO

Keywords:
Liver
Free-breathing
Multiphasic dynamic MRI
EOB
Compressed sensing

ABSTRACT

Purpose: To investigate the relationship between the hepatic contrast enhancement effect in the hepatobiliary phase (HBP) and the contrast enhancement parameters based on the data of continuous signal changes in free-breathing multiphasic dynamic EOB-MR imaging using a compressed sensing (CS) and the self-gating technique, and to clarify which contrast enhancement parameters are useful for estimating the hepatic enhancement effect in the HPB.

Method: This study included 96 patients. The contrast enhancement ratio (CER) of the liver parenchyma from phase x to phase y was calculated as follows: $CER_{y\text{-}x}$: $(SI_y - SI_x)/SI_x$. The gradient of the regression line (GRL) was also calculated. Patients can be divided into two groups with sufficient or insufficient liver enhancement in the HBP, then each parameter was compared between these two groups.

Results: In the analysis of the arterioportal phases, $CER_{7\text{-}pre}$ in the sufficient HBP enhancement group was significantly higher than that in the insufficient HBP enhancement group (0.50 vs 0.44, $p < 0.001$). Regarding 5 min early hepatocyte phase (phases 1–28) analysis, significant differences were observed in $CER_{28\text{-}pre}$, $CER_{28\text{-}7}$ and $Gradient_{28\text{-}7}$ between the two groups (0.64 vs 0.47, 0.10 vs 0.03, 1.27 vs 0.27, all $p < 0.001$). For the strength of correlation, $CER_{7\text{-}pre}$, $CER_{28\text{-}pre}$, $CER_{28\text{-}7}$, and $GRL_{28\text{-}7}$ had higher correlation coefficients, compared with the blood sampling data.

Conclusion: CER in the arterio-portal phase and 5 min early hepatocyte phase had significant correlation with hepatic contrast enhancement effects in the 20 min HBP, suggesting that sufficient 20 min HBP enhancement may be estimated by the CER in the portal phase and 5 min early hepatocyte phase.

1. Introduction

In liver MR imaging using gadolinium ethoxybenzyl diethylenetriamine pentaacetic acid (Gd-EOB-DTPA; EOB), multiphasic dynamic imaging, including arterial, portal, transitional and hepatobiliary phases during a separate breath-hold has been widely used to detect and characterize hepatic lesions [1–3]. Additionally, some studies have shown that the signal intensity (SI) of the hepatic parenchyma in the hepatobiliary phase (HBP) was related to the severity of hepatic fibrosis and could be used to estimate the liver function [4,5]. However, there have been several drawbacks in multiphasic dynamic MR imaging obtained during a separate breath-hold. For instance, transient respiratory motion artifacts have often been reported in arterial-phase imaging after the administration of EOB [6–8]. At the same time, the detection of early enhancement in hypervascular hepatic nodules has been sometimes hampered by the relatively short arterial window and inappropriate scan timing [9,10]. In addition, it was not possible to evaluate the continuous hemodynamic changes of the hepatic parenchyma or hepatic lesions from the arterial phase to the early HBP.

Recently, with the introduction of compressed sensing (CS) and the self-gating technique, continuous multiphase dynamic MR imaging for several minutes during free breathing has become possible [9,11,12]. Some studies have reported that this technique would be an alternative to standard breath-hold dynamic MR sequences in patients who cannot

* Corresponding author at: Department of Radiology, Yamaguchi University Graduate School of Medicine, 1-1-1 Minami-Kogushi, Ube, Yamaguchi 755-8505, Japan.
E-mail address: tanabe.m@yamaguchi-u.ac.jp (M. Tanabe).

https://doi.org/10.1016/j.ejrad.2021.109959
Received 17 May 2021; Received in revised form 30 August 2021; Accepted 15 September 2021
Available online 20 September 2021

hold their breath [9,11,12]. Furthermore, it allows for the evaluation of the continuous signal change of the hepatic parenchyma over time from the early arterial phase to the early hepatocyte phase. The purpose of this study was to investigate the relationship between the hepatic contrast enhancement effect in the HBP and the hepatic contrast enhancement parameters based on the data of continuous signal changes obtained by free-breathing continuous multiphasic dynamic EOB-MR imaging using CS and the self-gating technique, and to clarify which contrast enhancement parameters are useful for estimating the hepatic enhancement effect in the HPB in comparison to other factors, including blood sampling data.

2. Materials and methods

2.1. Study population

The present study received approval from our institutional review board, and the requirement of written informed consent for this retrospective data analysis was waived. Our radiology database was searched for cases involving patients with suspected liver disease who underwent hepatic MR examinations from June 1, 2018 to October 31, 2018. The inclusion criteria were as follows: 1) age > 20 years, 2) free-breathing continuous multiphasic dynamic MR imaging of the liver using CS and the self-gating technique, and 3) the use of EOB as a contrast agent. Patients with severe artifacts associated with body movements (other than breathing) (n = 3) and patients in whom the liver tumors occupied a large part of the liver (n = 3) were excluded because the measurement of the SI of the liver parenchyma was difficult or would be inaccurate. The final study population included 96 consecutive patients (male, n = 58; female, n = 38; median age: 69 years; range: 41–88 years) who received free-breathing continuous multiphasic dynamic EOB-MR imaging of the liver using CS and the self-gating technique (Fig. 1). MR examinations were indicated for the further evaluation of suspected liver lesions, including hepatocellular carcinoma (HCC) (n = 58), hemangioma (n = 2), liver metastasis (n = 24), cholangiocellular carcinoma (CCC) (n = 3), gallbladder carcinoma (n = 1), combined hepatocellular-cholangiocellular carcinoma (n = 3), malignant lymphoma (n = 2), and abscess (n = 1), and for the further investigation of liver dysfunction (n = 2).

2.2. MRI technique

MR examinations were performed on 3 T clinical systems (MAGNETOM Skyra, Siemens Healthineers, Germany). Free-breathing continuous multiphasic dynamic EOB-MR imaging of the entire liver using CS and the self-gating technique was performed using three-dimensional T1-weighted (3D) gradient echo with the fat suppression technique using the following parameters: repetition time/echo time (TR/TE) 3.92/1.4 msec, flip angle 10°, thickness 2.5 mm, 90% rectangular field of view (FOV) adapted to patient size, matrix 320 × 270, number of excitations (NEX) 1, and bandwidth 400 mHz/per pixel. Free-breathing continuous dynamic images were obtained every 11 s for approximately 5 min including 1 pre-contrast and 28 subsequent post-contrast phases. Just after the completion of the pre-contrast phase acquisition, the injection of EOB (0.1 mg/kg, Primovist; Bayer Healthcare, Berlin, Germany) was started at a rate of 1.0 mL/sec using a power injector followed by flushing with 20 mL of saline. At the same time, the first post-contrast phase acquisition was started to obtain continuous multiphasic dynamic MR images (28 phases). Finally, HBP images were separately obtained 20 min after contrast injection as 29th phase images.

2.3. Image analysis

The region of interest (ROI) was set as large as possible at two locations in the right lobe and one in the left lobe to measure the SI in each phase of images at the same location. The average SI values of the three ROIs in each phase were used for the data analysis. Several contrast enhancement parameters based on these SI data measured in each phase were calculated to evaluate the enhancement effects of the liver parenchyma, reflecting continuous signal changes. The following contrast enhancement parameters were evaluated. First, the contrast enhancement ratio (CER) from phase x to phase y was calculated as follows: $CER_{y\text{-}x}$: $(SI_y - SI_x)/SI_x$. We calculated $CER_{4\text{-}pre}$ (arterial enhancement rate), $CER_{7\text{-}5}$ (portal-arterial enhancement rate), $CER_{7\text{-}pre}$ (portal enhancement rate), $CER_{28\text{-}pre}$ (5 min early hepatocyte enhancement rate), $CER_{28\text{-}7}$ (early hepatocyte-portal enhancement rate), and $CER_{HBP\text{-}pre}$ (20 min hepatocyte enhancement rate). Next, the gradient of the regression line (GRL) from phase x to phase y ($GRL_{y\text{-}x}$) was calculated. $GRL_{y\text{-}x}$ calculated were as follows: $GRL_{4\text{-}2}$ (arterial transit gradient), $GRL_{7\text{-}4}$ (portal transit gradient), $GRL_{7\text{-}2}$ (arterioportal transit gradient), $GRL_{28\text{-}7}$ (early hepatocytic transit gradient). Regarding the arterial transit gradient, we calculated $GRL_{4\text{-}2}$ rather than $GRL_{4\text{-}1}$ to more accurately evaluate the arterial transit of the liver parenchyma, since there was little change in the SI of the liver parenchyma from phase 1 to phase 2 due to the minimal inflow of contrast medium into the liver parenchyma. A previous study showed that, according to the severity of liver fibrosis (F0-F2 vs. F3-F4), patients could be divided into two groups with sufficient or insufficient liver enhancement in the HBP based on $CER_{HBP\text{-}pre}$ with a cutoff value of 0.703 [13]. Then, the CER and GRL

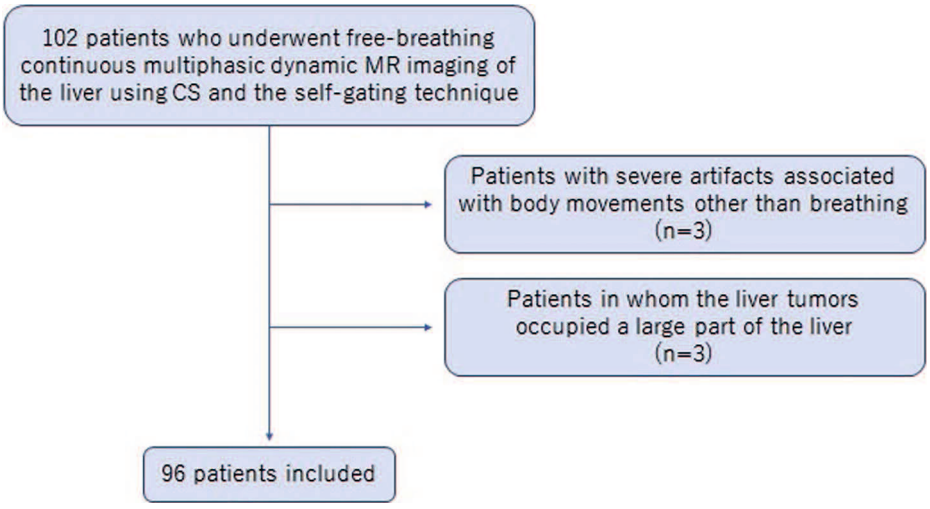

Fig. 1. Patient inclusion flowchart for this study. CS = compressed sensing.

values were compared between the sufficient HBP enhancement group and the insufficient HBP enhancement group. In addition, other parameters, including age, sex, total bilirubin, prothrombin time, albumin, and eGFR were also compared between the two groups.

2.4. Statistical analysis

Variables were assessed for normal distribution using the Shapiro-Wilk test. Continuous variables were compared between two groups using the Mann-Whitney *U* test, and categorical variables were compared using chi-squared test. Spearman's rank correlation coefficients were used to investigate relationships between the hepatic contrast enhancement effect in the HBP and each parameter. P values of < 0.05 were considered to indicate statistical significance. The JMP Pro 14 software program (SAS Institute Inc., Cary, NC, USA) was used to perform the statistical analyses.

3. Results

Based on a cutoff value of 0.703 in $CER_{HBP\text{-}pre}$, as reported in the previous study [13], 52 patients were categorized in the sufficient HBP enhancement group while 44 patients were in the insufficient HBP enhancement group. The sufficient HBP enhancement group included 6 patients with cirrhosis (Child-Pugh class A, n = 3; B, n = 3; and C, n = 0) and 20 patients with chronic hepatitis, while the insufficient HBP enhancement group included 13 patients with cirrhosis (Child-Pugh class A, n = 8; B, n = 5; and C, n = 0) and 16 patients with chronic hepatitis. The results of the differences in each parameter between the sufficient HBP enhancement group and the insufficient HBP enhancement group are shown in Table 1. In the analysis of the arterioportal phases (phases 1–7), $CER_{7\text{-}pre}$ in the sufficient HBP enhancement group was significantly higher than that in the insufficient HBP enhancement group (median: 0.50 vs. 0.43, $p < 0.01$) while the differences in $CER_{4\text{-}pre}$, $GRL_{4\text{-}2}$, $GRL_{7\text{-}4}$ and $GRL_{7\text{-}2}$ between the two groups were not statistically significant.

Regarding the analysis of the 5-min early hepatocyte phase (phases 1–28), significant differences were observed between the sufficient HBP enhancement group and the insufficient HBP enhancement group in $CER_{28\text{-}pre}$, $CER_{28\text{-}7}$ and $GRL_{28\text{-}7}$ (median: 0.64 vs. 0.47, 0.10 vs. 0.02, 0.11 vs. 0.02, respectively; all $p < 0.01$) (Figs. 2, 3). Significant differences were also observed in total bilirubin, albumin, prothrombin time, and eGFR (blood sampling parameters; median values: 0.6 vs. 0.8, $p = 0.02$; 4.2 vs. 4.0, $p < 0.01$; 100.9 vs. 91.7, $p = 0.04$; and 68.5 vs. 74.6, $p < 0.01$, respectively) and in the presence of cirrhosis ($p = 0.02$). However, there was no significant differences in age or sex between the two groups ($p = 0.98$ and $p = 0.21$ respectively).

Regarding the strength of correlation between the hepatic contrast enhancement effect in the HBP and each parameter, $CER_{7\text{-}pre}$, $CER_{28\text{-}pre}$, $CER_{28\text{-}7}$, $GRL_{7\text{-}2}$, and $GRL_{28\text{-}7}$ showed a significant positive correlation with HBP enhancement, and had comparable or higher correlation coefficients in comparison to total bilirubin, prothrombin time, albumin, and eGFR. $CER_{28\text{-}pre}$ showed the highest correlation coefficient (0.83) (Table 2).

Table 1
Comparison of each contrast enhancement parameter and other factors between the sufficient HBP enhancement group and the insufficient HBP enhancement group.

	Sufficient HBP enhancement (n = 52)	Insufficient HBP enhancement (n = 44)	*p* value
$CER_{4\text{-}pre}$ *	0.16 (0.18)	0.18 (0.16)	0.74
$CER_{7\text{-}4}$ *	0.24 (0.18)	0.19 (0.10)	0.06
$CER_{7\text{-}pre}$ *	0.50 (0.13)	0.43 (0.12)	<0.01
$CER_{28\text{-}pre}$ *	0.64 (0.13)	0.47 (0.10)	<0.01
$CER_{28\text{-}7}$ *	0.10 (0.07)	0.02 (0.08)	<0.01
$GRL_{4\text{-}2}$ (/sec) *	1.55 (1.81)	1.57 (1.67)	0.68
$GRL_{7\text{-}4}$ (/sec) *	1.88 (1.31)	1.51 (0.92)	0.11
$GRL_{7\text{-}2}$ (/sec) *	2.07 (0.73)	1.84 (0.71)	0.07
$GRL_{28\text{-}7}$ (/sec) *	0.11 (0.07)	0.02 (0.98)	<0.01
Total bilirubin (mg/dL) *	0.6 (0.47)	0.8 (0.50)	0.02
Albumin (g/dL) *	4.2 (0.47)	4.0 (0.77)	<0.01
Prothrombin time (%) *	100.9 (21.8)	91.7 (29.0)	0.04
eGFR (mL/min/1.73 m^2) *	68.5 (22.9)	74.6 (29.1)	<0.01
Age (years) *	69 (13)	69 (13)	0.98
No. of men †	26 (50)	32 (72)	0.21
No. of cirrhosis †	6 (11)	13 (29)	0.02

* Data are the median, with interquartile rang in parentheses. *P* value was calculated with the Mann-Whitney *U* test.

† Data are number of patients, with the percentage in parentheses. *P* value was calculated with the chi-square test.

4. Discussion

In this study, there were significant positive correlations between HBP enhancement and $CER_{7\text{-}pre}$, $CER_{28\text{-}pre}$, $CER_{28\text{-}7}$, $GRL_{7\text{-}2}$, and $GRL_{28\text{-}7}$, showing that hepatic signal changes over time during the arterioportal and early hepatocyte phases were associated with hepatic contrast enhancement in the HBP. It has been reported that in EOB-MRI, hepatic contrast enhancement in the HBP was related to the liver function, as estimated by the data of several blood sampling parameters [4,5,14]. The results for eGFR, total bilirubin, albumin, and prothrombin time in this study were generally significantly correlated with the hepatic contrast enhancement in the HBP, which is consistent with previous studies [14–16]. However, the correlation coefficients were 0.43 for $CER_{7\text{-}pre}$, 0.83 for $CER_{28\text{-}pre}$, 0.56 for $CER_{28\text{-}7}$ and 0.58 for $GRL_{28\text{-}7}$, which were higher in comparison to the blood sampling data. Therefore, it would be more accurate to analyze the data obtained during free-breathing continuous multiphasic dynamic imaging rather than using blood sampling data for the estimation of hepatic contrast enhancement in the HBP.

The analysis of the early hepatocyte phase (phases 7 to 28) showed that $CER_{28\text{-}7}$ and $GRL_{28\text{-}7}$ were significantly higher in the sufficient HBP enhancement group than in the insufficient HBP enhancement group. This finding indicated that the decreased uptake of EOB into hepatocytes occurred within 5 min, during the early hepatocyte phase, leading to insufficient EOB enhancement in the HBP (20 min). Additionally, in the analysis of the arterio-portal phase (phases 1 to 7), $CER_{7\text{-}pre}$ in the sufficient HBP enhancement group was significantly higher in comparison to the insufficient HBP enhancement group, and $CER_{7\text{-}4}$ and $GRL_{7\text{-}2}$ tended to be higher in the sufficient HBP enhancement group in comparison to the insufficient HBP enhancement group. These results suggested that insufficient HBP enhancement would have a causative

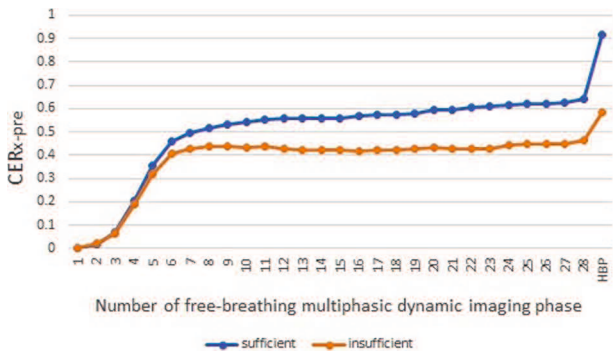

Fig. 2. Comparison of signal change of the hepatic parenchyma over time between the sufficient HBP enhancement group and the insufficient HBP enhancement group. Note: $CER_{x\text{-}pre} = (SI_x - SI_{pre})/SI_{pre}$, CER = contrast enhancement ratio, SI_x = signal intensity of the liver on phase X (X: 1–28, HBP), SI_{pre} = signal intensity of the liver on precontrast phase.

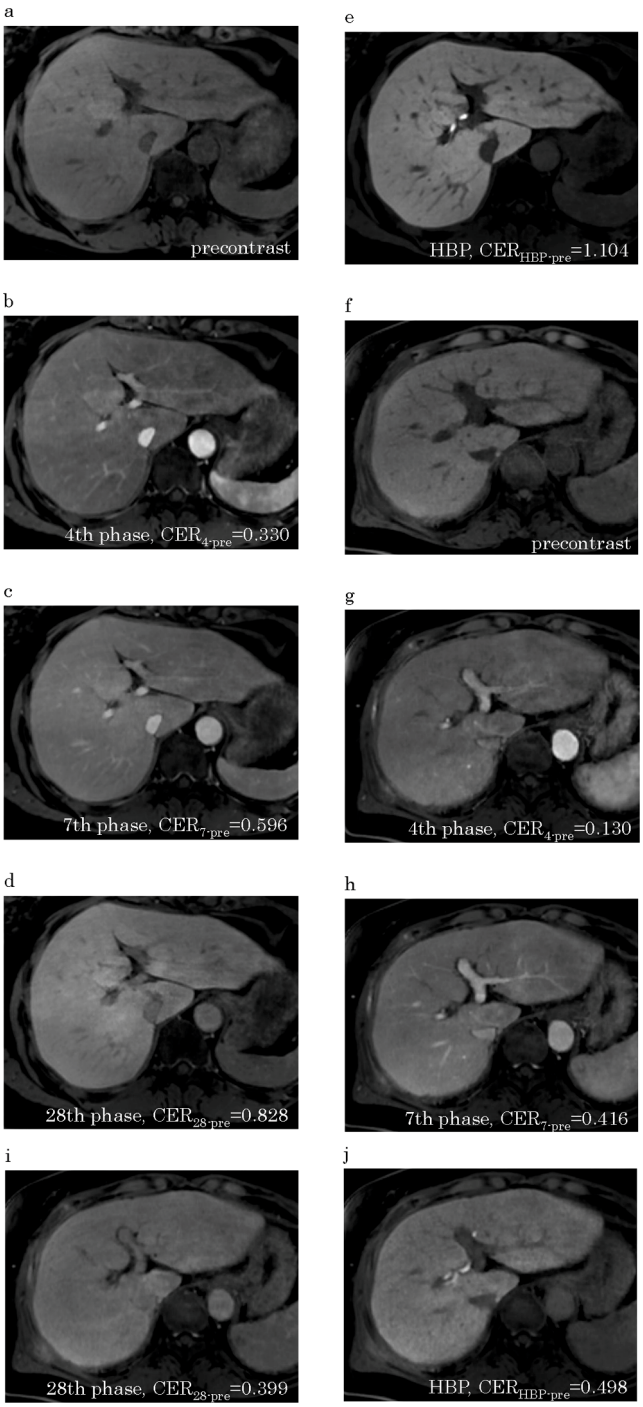

Fig. 3. Free-breathing continuous multiphasic dynamic EOB-MR images using CS and self-gating technique. (a)-(e) Precontrast (a), 4th (b), 7th (c), 28th (d) phases and HBP (e) images in a 65-year-old woman with sufficient HBP enhancement of the liver. (f)-(j) Precontrast (f), 4th (g), 7th (h), 28th (i) phases and HBP (j) images in an 86-year-old woman with insufficient HBP enhancement of the liver. The values of $CER_{4\text{-}pre}$, $CER_{7\text{-}pre}$, $CER_{28\text{-}pre}$ and $CER_{HBP\text{-}pre}$ in these two patients were shown in the Figures.

association with the decreased portal venous flow, probably due to underlying cirrhosis, which induces the reduced hepatic uptake of EOB, and suggested the clinical value of free-breathing multiphasic dynamic imaging in evaluating continuous signal changes of the liver from the arterio-portal phase to early hepatocyte phase.

In EOB-MRI, the standard delay time of 20 min for the HBP has been used in many facilities. However, it would be clinically better to shorten this delay time if sufficient hepatic enhancement can be assured. From this point of view, using the data obtained in our study, it may be possible to reduce the delay time of imaging in the HBP more accurately in comparison to the accuracy that could be achieved using the Child-Pugh score or blood sampling data, depending on the individual case. Since only one HBP was obtained in our study, it was not possible to clarify exactly how much the time required for imaging in the HBP could be reduced. Further research is necessary to clarify this issue.

Table 2
Correlation between hepatic contrast enhancement effect in the HBP and each parameter.

	Spearman rank correlation coefficient	*p* value
$CER_{4\text{-}pre}$	0.14	0.15
$CER_{7\text{-}4}$	0.17	0.08
$CER_{7\text{-}pre}$	0.43	<0.01
$CER_{28\text{-}pre}$	0.83	<0.01
$CER_{28\text{-}7}$	0.56	<0.01
$GRL_{4\text{-}2}$ (/sec)	0.12	0.22
$GRL_{7\text{-}4}$ (/sec)	0.15	0.13
$GRL_{7\text{-}2}$ (/sec)	0.22	0.02
$GRL_{28\text{-}7}$ (/sec)	0.58	<0.01
eGFR (mL/min/1.73 m^2)	−0.23	0.02
Total bilirubin (mg/dL)	−0.27	<0.01
Albumin (g/dL)	0.31	<0.01
Prothrombin time (%)	0.20	0.04
Age (years)	0.06	0.51

The present study was associated with some limitations. First, the retrospective design inevitably involves a potential bias. Second, the study cohort was a heterogeneous patient population that included patients with chronic hepatitis, cirrhosis, and non-cirrhosis. Third, we used a relatively long acquisition time of 11 s in each phase of free-breathing dynamic imaging to ensure image quality. A shorter acquisition time would be desirable in future studies. Fourth, the detection or visualization of hepatic lesions in the HBP was not evaluated, and thus, we cannot describe the influence of hepatic contrast enhancement in the HBP on the detection of hepatic lesions. However, this study was mainly designed to assess the relationship between continuous signal changes of the liver and the contrast enhancement effect in the HBP, and the prediction of sufficient HBP enhancement would help yield better visualization of hepatic lesions. Finally, we did not obtain free-breathing dynamic imaging data from 5 to 20 min, but it is not realistic to store these huge volumes of data in clinical practice.

5. Conclusion

In conclusion, in the analysis of hepatic contrast enhancement parameters based on the continuous data of the signal changes over time obtained by free-breathing continuous multiphasic dynamic EOB-MR imaging using CS and the self-gating technique, CER in the arterio-portal phase and the early hepatocyte phase (5 min) had significant correlation with hepatic contrast enhancement effects in the HBP (20 min), and showed significant difference between sufficient and insufficient HBP enhancement groups, suggesting that sufficient HBP (20 min) enhancement may be estimated by the CER in the arterio-portal phase and the early hepatocyte phase (5 min).

CRediT authorship contribution statement

Masaya Tanabe: Data curation, Formal analysis, Writing – original draft. **Masahiro Tanabe:** Methodology, Formal analysis, Writing – review & editing. **Matakazu Furukawa:** Writing – review & editing. **Etsushi Iida:** Investigation. **Munemasa Okada:** Writing – review & editing. **Katsuyoshi Ito:** Conceptualization, Writing – review & editing, Supervision.

Declaration of Competing Interest

The authors declare that they have no known competing financial interests or personal relationships that could have appeared to influence the work reported in this paper.

References

[1] A. Kitao, Y. Zen, O. Matsui, T. Gabata, S. Kobayashi, W. Koda, K. Kozaka, N. Yoneda, T. Yamashita, S. Kaneko, Y. Nakanuma, Hepatocellular carcinoma: signal intensity at gadoxetic acid-enhanced MR Imaging–correlation with molecular transporters and histopathologic features, Radiology 256 (3) (2010) 817–826.

[2] S. Nakao, M. Tanabe, M. Okada, M. Furukawa, E. Iida, K. Miyoshi, N. Matsunaga, K. Ito, Liver imaging reporting and data system (LI-RADS) v2018: comparison between computed tomography and gadoxetic acid-enhanced magnetic resonance imaging, Jpn. J. Radiol. 37 (9) (2019) 651–659.

[3] S. Semaan, N. Vietti Violi, S. Lewis, M. Chatterji, C. Song, C. Besa, J.S. Babb, M. I. Fiel, M. Schwartz, S. Thung, C.B. Sirlin, B. Taouli, Hepatocellular carcinoma detection in liver cirrhosis: diagnostic performance of contrast-enhanced CT vs. MRI with extracellular contrast vs. gadoxetic acid, Eur. Radiol. 30 (2) (2020) 1020–1030.

[4] Y.-H. Chuang, H.-Y. Ou, M.Z. Lazo, C.-L. Chen, M.-H. Chen, C.-C. Weng, Y.-F. Cheng, Predicting post-hepatectomy liver failure by combined volumetric, functional MR image and laboratory analysis, Liver Int. 38 (5) (2018) 868–874.

[5] K. Sandrasegaran, E. Cui, R. Elkady, P. Gasparis, G. Borthakur, M. Tann, S. Liangpunsakul, Can functional parameters from hepatobiliary phase of gadoxetate MRI predict clinical outcomes in patients with cirrhosis? Eur. Radiol. 28 (10) (2018) 4215–4224.

[6] M.S. Davenport, M.R. Bashir, J.A. Pietryga, J.T. Weber, S. Khalatbari, H.K. Hussain, Dose-toxicity relationship of gadoxetate disodium and transient severe respiratory motion artifact, AJR Am. J. Roentgenol. 203 (4) (2014) 796–802.

[7] S. Ichikawa, U. Motosugi, K. Sato, T. Shimizu, T. Wakayama, H. Onishi, Transient Respiratory-motion Artifact and Scan Timing during the Arterial Phase of Gadoxetate Disodium-enhanced MR Imaging: The Benefit of Shortened Acquisition and Multiple Arterial Phase Acquisition, Magn. Reson. Med. Sci. 20 (3) (2021) 280–289.

[8] M. Tanabe, M. Higashi, E. Iida, H. Onoda, K. Ihara, S. Ariyoshi, F. Kameda, K. Miyoshi, M. Furukawa, M. Okada, K. Ito, Transient respiratory motion artifacts in multiple arterial phases on abdominal dynamic magnetic resonance imaging: a comparison using gadoxetate disodium and gadobutrol, Jpn. J. Radiol. 39 (2) (2021) 178–185.

[9] J.H. Yoon, M.H. Yu, W. Chang, J.-Y. Park, M.D. Nickel, Y. Son, B. Kiefer, J.M. Lee, Clinical Feasibility of Free-Breathing Dynamic T1-Weighted Imaging With Gadoxetic Acid-Enhanced Liver Magnetic Resonance Imaging Using a Combination of Variable Density Sampling and Compressed Sensing, Invest. Radiol. 52 (10) (2017) 596–604.

[10] C.J. Zech, B. Vos, A. Nordell, M. Urich, L. Blomqvist, J. Breuer, M.F. Reiser, H. J. Weinmann, Vascular enhancement in early dynamic liver MR imaging in an animal model: comparison of two injection regimen and two different doses Gd-EOB-DTPA (gadoxetic acid) with standard Gd-DTPA, Invest. Radiol. 44 (6) (2009) 305–310.

[11] H. Chandarana, L.i. Feng, T.K. Block, A.B. Rosenkrantz, R.P. Lim, J.S. Babb, D. K. Sodickson, R. Otazo, Free-breathing contrast-enhanced multiphase MRI of the liver using a combination of compressed sensing, parallel imaging, and golden-angle radial sampling, Invest. Radiol. 48 (1) (2013) 10–16.

[12] B. Kaltenbach, A.M. Bucher, J.L. Wichmann, D. Nickel, C. Polkowski, R. Hammerstingl, T.J. Vogl, B. Bodelle, Dynamic Liver Magnetic Resonance Imaging in Free-Breathing: Feasibility of a Cartesian T1-Weighted Acquisition Technique With Compressed Sensing and Additional Self-Navigation Signal for Hard-Gated and Motion-Resolved Reconstruction, Invest. Radiol. 52 (11) (2017) 708–714.

[13] C. Besa, M. Wagner, G. Lo, S. Gordic, M. Chatterji, P. Kennedy, A. Stueck, S. Thung, J. Babb, A. Smith, B. Taouli, Detection of liver fibrosis using qualitative and quantitative MR elastography compared to liver surface nodularity measurement, gadoxetic acid uptake, and serum markers, J. Magn. Reson. Imaging 47 (6) (2018) 1552–1561.

[14] S. Gschwend, W. Ebert, M. Schultze-Mosgau, J. Breuer, Pharmacokinetics and imaging properties of Gd-EOB-DTPA in patients with hepatic and renal impairment, Invest. Radiol. 46 (9) (2011) 556–566.

[15] M. Okada, T. Murakami, R. Kuwatsuru, Y. Nakamura, H. Isoda, S. Goshima, R. Hanaoka, H. Haradome, Y. Shinagawa, A. Kitao, Y. Fujinaga, N. Marugami, M. Yuki, T. Ichikawa, A. Higaki, M. Hori, S. Fujii, O. Matsui, Biochemical and Clinical Predictive Approach and Time Point Analysis of Hepatobiliary Phase Liver Enhancement on Gd-EOB-DTPA-enhanced MR Images: A Multicenter Study, Radiology 281 (2) (2016) 474–483.

[16] W. Zhang, X. Wang, Y. Miao, C. Hu, W. Zhao, Liver function correlates with liver-to-portal vein contrast ratio during the hepatobiliary phase with Gd-EOB-DTPA-enhanced MR at 3 Tesla, Abdom. Radiol. (NY) 43 (9) (2018) 2262–2269.